About Verification of Calculation Methods of the Shock Waves

Valentin Kuropatenko[1,2] and Elena Shestakovskaya[2]

[1] Russian Federal Nuclear Center-Zababakhin All–Russia Research Institute of Technical Physics,
456770, Snezhinsk, Russian Federation
[2] South Ural State University(National Research University),
454080, Chelyabinsk, Russian Federation
v.f.kuropatenko@yandex.ru, leshest@list.ru

Abstract. Mathematical modeling is now a key tool of research into dynamic processes in continuum mechanics. Each particular problem is solved with already existing or newly developed models and methods, whose properties are determined from a priori study into stability, approximation, monotonicity etc within linear approaches. The accuracy of difference schemes is mainly evaluated through comparison between calculated results and reference solutions. The paper discusses some problems which have analytical solutions. These are shock convergence, the dynamic compression of a gas sphere, and some problems with stationary shocks.

Keywords: shock, analytical solution, ideal gas, spherical symmetry, stationary shock

1 Introduction

The properties of difference schemes that approximate the conservation laws are often evaluated with a priori methods which involve studies into stability, approximation, monotonicity, conservatism, distraction etc. It should however be noted that most of these methods are developed for acoustic approximations and simple equations of state. In continuum mechanics, the properties of a mathematical model may notably differ from what linear theory predicts due to nonlinearities induced by real-world equations of state, shocks, plasticity and other material properties.

Linear theory looses its rigor when applied to nonlinear equations. The importance of the convergence theorem [1] is strongly exaggerated because it is still proved for linear equations and not for nonlinear ones, and real calculations are done not for vanishing but finite Δx and Δt. A very vivid discussion of stability and convergence criteria and their rigidity can be found in [2].

The calculation of shock waves strong discontinuities in all material properties requires special attention. On the shock surface the conservation laws take the form of nonlinear algebraic equations which relate the values of quantities across the shock. Entropy jumps as all the other functions do. This is the fundamental difference between a shock and a wave where the quantities vary continuously. Flows with shocks are often

simulated with homogeneous methods which treat the strong shock as a layer of a finite width comparable with the cell size. This ability of difference schemes is called distraction [3]. Since the states across the shock are related by the Hugoniot, there must be a mechanism which allows entropy to grow in the shock distraction region. Physical viscosity and heat conduction in continuum mechanics equations cannot give a distraction width of several cell sizes. The proposal by Neumann and Richtmyer to use a mathematical 'viscosity' [4] seems to resolve the problem. Their method has gained wide acceptance. Pseudo-viscosity is taken in different forms linear, quadratic, or linear-quadratic [4-7]. But the method does not ensure convergence to the exact solution if the form of pseudo-viscosity changes. So, the author of [8] gives an example where different schemes with different viscosities converge to different solutions in the limit. In [9], there is an example of spherical convergence where energy dissipation defined by pseudo-viscosity is shown to be several times higher than energy dissipation due to plasticity.

Advantages and disadvantages of a mathematical model can be seen from comparison between its predictions and analytical solutions. The paper discusses some problems which have exact analytical solutions. It gives their statements (initial and boundary conditions, equations of state, and physical parameters) and solutions in the form of formulas or tables. In order to verify performance of a difference scheme, one needs to solve the problem numerically and compare the result with the exact solution.

The problems are broken into two groups for stationary and non-stationary shocks. In problems with stationary shocks, derivatives in the exact solution are zero everywhere beyond the distraction zone and hence approximation errors are also zero. In the distraction zone, the derivatives and approximation errors reach high values. Here the strong shock is smeared over several cells where entropy differs. These problems help verify real shock distraction, monotonicity, entropy variation, and the dependence of calculated results on the relation between steps in space and time, and on cell size (the number of points in the mesh). All these properties reveal themselves differently for strong and weak shocks. Shock strength is characterized be the difference between pressures behind and before the shock.

In problems with non-stationary shocks, the derivatives and derivative-dependent approximation errors are high beyond the distraction zone. This group includes shock convergence and spherical shell convergence problems. In the last problem, the boundary conditions and released energy are adjusted so as to keep material density constant despite large pressure and velocity gradients.

Some analytical solutions are used for comparison with results obtained with the difference schemes which are based on the energy dissipation method described in [10-13].

2 Stationary shock

Consider a material with parameters P_0, V_0, E_0, U_0 which do not change with time. At a time t_0 its left boundary instantaneously starts moving at a constant positive velocity, producing a shock wave which propagates into the material. The equations

$$WV_+ + U_+ = WV_- + U_-, \tag{1}$$

$$WU_+ - P_+ = WU_- - P_-, \tag{2}$$

$$W\varepsilon_+ - P_+U_+ = W\varepsilon_- - P_-U_- \tag{3}$$

relate the material states $P_- = P_0,\ V_- = V_0,\ E_- = E_0,\ U_- = U_0$ with the state after the discontinuity $P = P_+,\ V = V_+,\ E = E_+,\ U = U_+$ before and behind the shock, and the shock velocity W. The number of quantities is larger than the number of equations (1) - (3) + equation of state. To solve this system of equations requires that one of the quantities be taken as parameter. Let it be U. Take the equation of state (EOS) for ideal gas in the form

$$PV = (\gamma - 1)\, E \tag{4}$$

and transform equations (1) - (3) to the dependence of P on U and other zero-subscripted quantities

$$P = P_0 + \frac{\gamma + 1}{4}\ \frac{\Delta U^2}{V_0} + \sqrt{\left(\frac{\gamma + 1}{4}\frac{\Delta U^2}{V_0}\right)^2 + \frac{\gamma P_0}{V_0}\ \Delta U^2}, \tag{5}$$

where $\Delta U = U - U_0$. From equations (1) - (3) and (5) we find P, W, V and E:

$$W = (P - P_0)/(U - U_0),\ V = V_0 - (U - U_0)/W,\ E = E_0 + 0,5\,(P + P_0)\,(V - V_0)\,. \tag{6}$$

For condense matter, a simple equation of state has the form

$$P = (n - 1)\,\rho E + C_{0k}^2\,(\rho - \rho_{0k})\,, \tag{7}$$

where $\rho = 1/V$ - is material density, ρ_{0k} - is its density at a point with coordinates $T = 0$, $P = 0$ and C_{0k} - is sound velocity at this point. For EOS (7) equations (1) - (3) transform to the Hugoniot equation

$$P = P_0 + \frac{n + 1}{4}\rho_0 \Delta U^2 + \sqrt{\left(\frac{\gamma + 1}{4}\rho_0 \Delta U^2\right)^2 + \rho_0 \Delta U^2 \left(nP_0 + \rho_{0k} C_{0k}^2\right)}. \tag{8}$$

Equations (6) for W, V, and E remain the same.

For convenience, we treat all quantities in equation (5) - (8) as dimensionless. That is why both in gas and in condense matter, the initial dimensionless density is unity. Conversion to density in g/cm^3 is done through multiplying by the constant used for conversion to dimensionless density. All the other quantities are treated similarly.

Problem 1. Strong shock in monatomic gas. At $t = 0$, a region $0 \le x_0 \le 1$ is occupied with gas described by EOS (4) with parameters $\gamma = 5/3$, $P_0 = 0$, $\rho_0 = 1$, $E_0 = 0$, $U_0 = 0$. Here x_0 – is the Eulerian coordinate at $t = 0$. In Lagrangian difference schemes x_0 is a Lagrangian coordinate. At $t > 0$, $U = 1$ is specified on the left boundary ($x_0 = 0$) and $U = 0$ is on the right one ($x_0 = 1$).

The quantities behind the shock front and front velocity W are determined from equations (1) - (3): $\rho = 4$, $E = 0.5$, $P = 4/3$, $W = 4/3$. At $t = 0.375$, the shock is at a point $x_0 = 0.5$ and the analytical solution is determined by

$P = 1.33333, \quad \rho = 4.0, \quad E = 0.5, \quad U = 1.0, \quad$ for $x_0 \leq 0.5$, and

$P = 0, \qquad \rho = 1.0, \quad E = 0, \quad U = 0, \quad$ for $x_0 > 0.5$

Figures 1 and 2 depict $P(x_0)$ and $U(x_0)$ at $t = 0.575$. The solid lines show analytical solutions and the marked ones show calculations with the difference scheme from [12]. The calculations were done with a uniform mesh of $N = 100$ points in x_0 and Courant number 0.5.

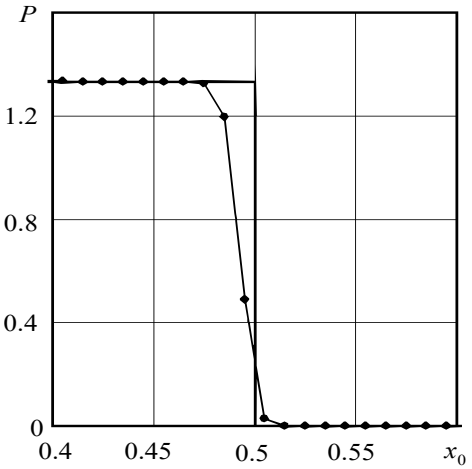

Fig. 1. Problem 1. $P(x_0)$ at $t = 0.375$

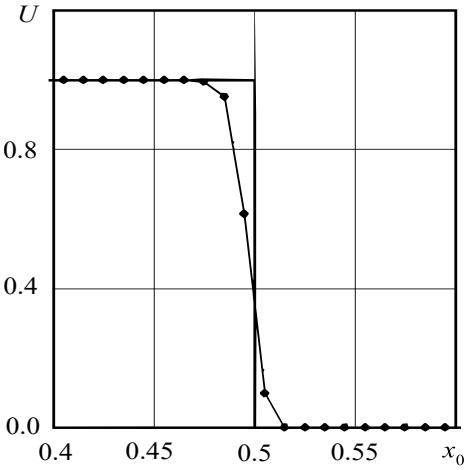

Fig. 2. Problem 1. $U(x_0)$ at time $t = 0.375$

Problem 2. Strong shock in monatomic gas described by EOS (4) and $\gamma = 1.25$ (ethylene). All the other parameters are the same as in Problem 1: $\rho_0 = 1$, $P_0 = 0$, $E_0 = 0$, $U_0 = 0$. The boundary conditions are also the same: $U(x_0 = 0, t) = 1$, $U(x_0 = 1, t) = 0$.

The quantities behind the shock front and front velocity are determined from equations (1) - (3): $\rho = 9$, $E = 0.5$, $P = 1.125$, $W = 1.125$. At $t = 0.44444$ the shock is at a point $x_0 = 0.5$, and the analytical solution is determined by

$P = 1.125, \quad \rho = 9.0, \quad E = 0.5, \quad U = 1 \quad$ for $x_0 \leq 0.5$, and

$P = 0, \qquad \rho = 1.0, \quad E = 0, \quad U = 0, \quad$ for $x_0 > 0.5$.

Figures 3 and 4 depict $P(x_0)$ and $U(x_0)$ at $t = 0.44444$. The solid lines show analytical solutions and the marked ones show calculations with the difference scheme from [12]. The calculations were done with a uniform mesh of $N = 100$ points in x_0 and Courant number 0.5.

Problem 3. The weak shock wave in monatomic gas. At $t = 0$, a region $0 \leq x_0 \leq 1$ is occupied with monatomic ideal gas described by EOS (4) with parameters $\gamma = 5/3$, $\rho_0 = 1$, $P_0 = 1$, $\rho_0 = 1$, $E_0 = 1.5$, $U_0 = 0$. At $t > 0$, $U = 0.5$ is specified on the left boundary ($x_0 = 0$) and $U = 0$ is on the right one ($x_0 = 1$). Behind the shock, $\rho = 1.428573$, $E = 1.925$, $P = 1.833333$, and $W = 1.666666$. The analytical solution at $t = 0.3$ is determined by

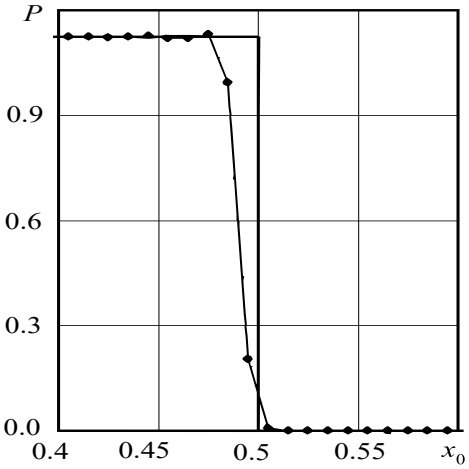

Fig. 3. Problem 2. $P(x_0)$ at $t = 0.44444$

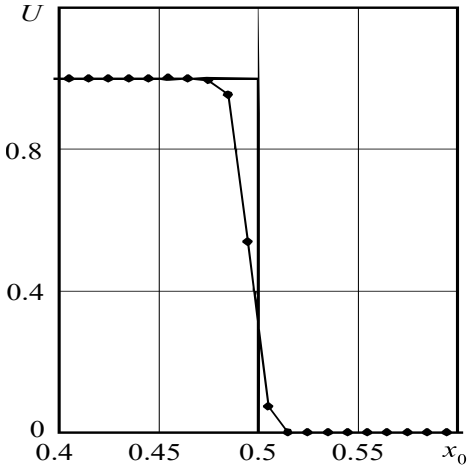

Fig. 4. Problem 2. $U(x_0)$ at $t = 0.44444$

$P = 1.83333, \quad \rho = 1.42857, \quad E = 1.925, \quad U = 0.5 \quad$ for $x_0 \leq 0.5$, and

$P = 1.0, \quad \rho = 1.0, \quad E = 1.50, \quad U = 0 \quad$ for $x_0 > 0.5$.

Figures 5 and 6 depict $P(x_0)$ and $U(x_0)$ at $t = 0.3$. The solid lines show analytical solutions and the marked ones show calculations with the difference scheme from [13]. The calculations were done with a uniform mesh of $N = 100$ points in x_0 and Courant number 0.5.

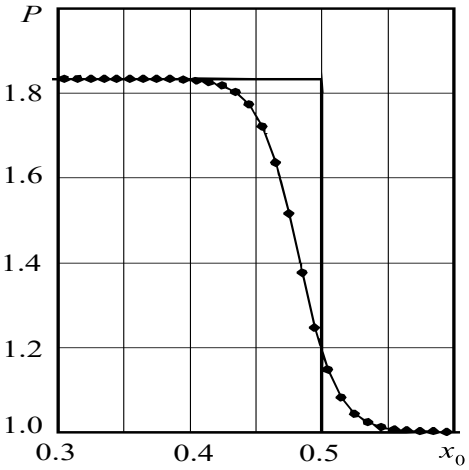

Fig. 5. Problem 3. $P(x_0)$ at $t = 0.3$

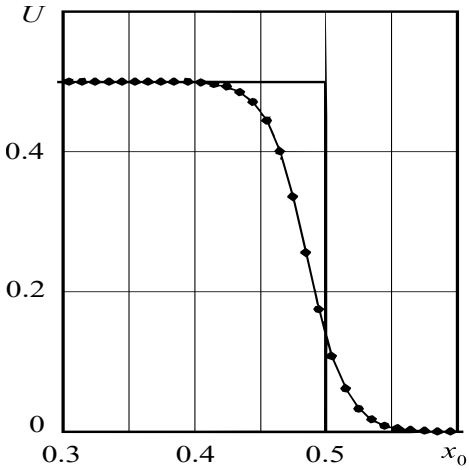

Fig. 6. Problem 3. $U(x_0)$ at $t = 0.3$

Problem 4. Strong shock in condense matter. At $t = 0$, a region $0 \le x_0 \le 1$ is occupied with condense matter described by EOS (7) which at $\rho_{0k} = 1$ and $C_{0k} = 1$ takes the form

$$P = (n-1)\rho E + \rho - 1, \tag{9}$$

At $t = 0$, the parameters are $\rho_0 = 1$, $E_0 = 0$, $P_0 = 0$, $U_0 = 0$, $n = 3$. For $t > 0$, $U = 2$ is specified on the left boundary ($x_0 = 0$) and $U = 0$ is on the right one ($x_0 = 1$). The equation for P is obtained from (8):

$$P = \frac{n+1}{4}\rho_0 U^2 + \sqrt{\left(\frac{n+1}{4}\rho_0 U^2\right)^2 + \rho_0 U^2}.$$

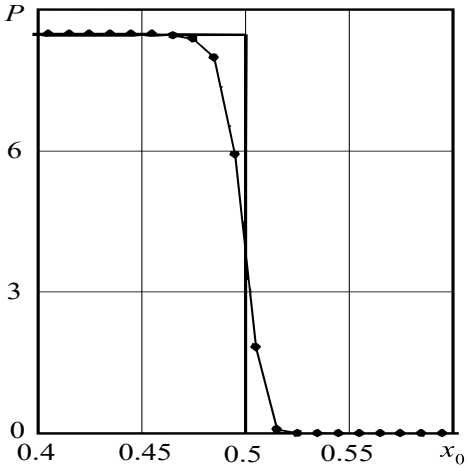

Fig. 7. Problem 4. $P(x_0)$ at $t = 0.118034$

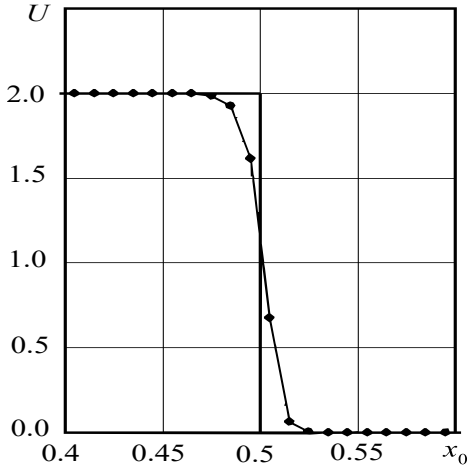

Fig. 8. Problem 4. $U(x_0)$ at $t = 0.118034$

The analytical solution at t = 0.118034 is determined by

$P = 8.47214$, $\rho = 1.89443$, $E = 2.0$, $U = 2.0$ for $x \le 0.5$, and

$P = 0$, $\rho = 1.0$, $E = 0$, $U = 0$ for $x > 0.5$.

Figures 7 and 8 depict $P(x_0)$ and $U(x_0)$ at $t = 0.118034$. The solid lines show analytical solutions and the marked ones show calculations with the difference scheme from [13]. The calculations were done with a uniform mesh of $N = 100$ points in x_0 and Courant number 0.5.

Problem 5. Weak shock in condense matter. At $t = 0$, a region $0 \le x_0 \le 1$ is occupied with a material described by EOS (9) with parameters: $\rho_0 = 1$, $E_0 = 2$, $P_0 = 4$, $U_0 = 0$, $n = 3$. For $t > 0$, $U = 1$ on the left boundary and $U = 0$ on the right one.

The analytical solution at $t = 0.105448$ is determined by

$P = 8.74166$, $\rho = 1.26726$, $E = 3.34359$, $U = 1.0$ for $x_0 \le 0.5$, and

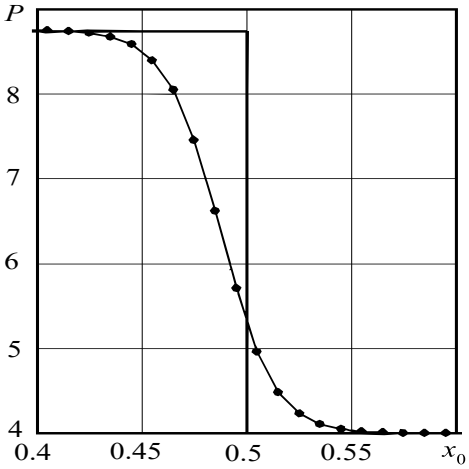

Fig. 9. Problem 5. $P(x_0)$ at $t = 0.105448$

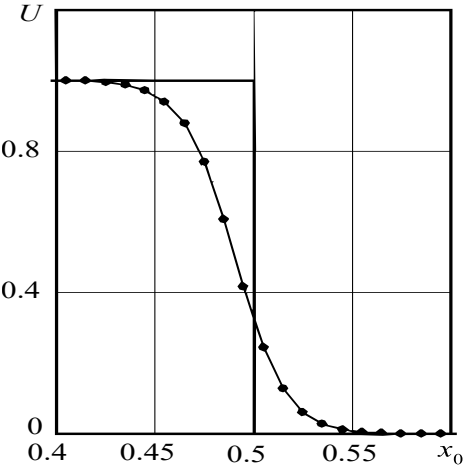

Fig. 10. Problem 5. $U(x_0)$ at $t = 0.105448$

$P = 4.0, \qquad \rho = 1.0, \qquad E = 2.0, \qquad U = 0 \qquad$ for $x_0 > 0.5$.

Figures 9 and 10 depict $P(x_0)$ and $U(x_0)$ at $t = 0.105448$. The solid lines show analytical solutions and the marked ones show calculations with the difference scheme from [13]. The calculations were done with a uniform mesh of $N = 100$ points in x_0 and Courant number 0.5.

3 The motion of a spherical layer of compressible ideal fluid

The problem of bubble collapse in fluid, or spherical shell convergence, arises in connection with cavitation corrosion of propellers. Solutions to the problem can be found in [14-16]. The full continuum mechanics model for 1D spherically symmetric flow of ideal compressible continua includes mass conservation, motion and internal energy equations:

$$\frac{\partial V}{\partial t} - 4\pi \frac{\partial r^2 U}{\partial M} = 0, \tag{10}$$

$$\frac{\partial U}{\partial t} + 4\pi r^2 \frac{\partial P}{\partial M} = 0, \tag{11}$$

$$\frac{\partial E}{\partial t} + P \frac{\partial V}{\partial t} = 0. \tag{12}$$

Equations (10)–(12) are written in Lagrangian coordinates. Here the partial derivatives with respect to time are substantial derivatives.

There no incompressible matter in nature. Mechanics simply considers a wide class of flows where density remains constant in time. Density constancy is often understood as incompressibility, i.e., $\beta_s = 0$ and $C^2 = \infty$. It is not true. The property of flow is not the property of matter.

As a rule [16], the models of 'incompressible' fluid do not include the energy conservation law and the equation of state. This makes them internally contradictive. As follows from (12), in ideal compressible fluid, $E = const$ at $V = const$. But in this case from the equation of state $P = P(V, E)$ we obtain that $P = const$, too. So, on the one hand, P varies, and on the other hand, P is constant. This contradiction can be removed if assume that fluid is not adiabatic, i.e., there is a source of energy in it. Then equation (12) is written as

$$\frac{\partial E}{\partial t} = -P\frac{\partial V}{\partial t} + \frac{\partial q}{\partial t}. \tag{13}$$

Equations (10), (11) and (13) allow solutions where density is constant. To keep the density of fluid constant requires energy. As follows from the theory of equations of state [17], in fluid, thermal pressure and energy, P_T and E_T, are related by the equation $P_T V = \Gamma(V)E_T$. Hereafter for $V = const$ the equation is taken in the form

$$PV_0 = \Gamma E, \tag{14}$$

where $\Gamma = const$, $P = P_T$, $E = E_T$. Since $P(t, M)$ is a solution to equations (11) and (12), then the dependence $E(t, M)$ which follows from (13) is quite specific in each flow. It is defined by the necessity of meeting the condition $V = const$.

Here we limit ourselves to flows where specific volume is independent of either M, or t, i.e., $V = const$. Also, we assume that fluid is compressible, i.e., its compressibility β_S is nonzero.

For $V = V_0$, the equation that relates the Eulearian coordinate r and the Lagrangian coordinate $dM = \left(4\pi r^2 \middle/ V_0\right) dr$ can be integrated from $M = 0$ at $r = r_B$ to an arbitrary finite M

$$r = \left(r_B^3 + 3V_0 M/4\pi\right)^{1/3}. \tag{15}$$

Here r_B is the time dependent coordinate of the bubble boundary. At $V = V_0$, equation (10) has the solution

$$r^2 U = f(t). \tag{16}$$

Since f is independent of M, equations (15) and (16) are valid for arbitrary M. On the bubble boundary where $M = 0$, equation (16) takes the form

$$r_B^2 U_B = f(t), \qquad U = U_B \frac{r_B^2}{r^2}. \tag{17}$$

where U_B is bubble boundary velocity.

Find U_B from (17) and substitute in the bubble boundary motion equation

$$\left(\frac{dr_B}{dt}\right)_M = U_B. \tag{18}$$

Integrate (18) together with (15), to obtain the dependence of r_B on t

$$r_B = \left(r_{B0}^3 + \int_{t_0}^{t} 3f(t)\,dt \right)^{1/3}. \tag{19}$$

It is seen from (17) and (19) that the motion of the bubble boundary is completely defined by $f(t)$. If $f(t) < 0$, then $U_B < 0$ too, i.e., the bubble collapses. The boundary convergence time tf is found from (19) at $r_B = 0$

$$r_{B0}^3 + \int_{t_0}^{t_f} 3f(t)\,dt = 0. \tag{20}$$

Following [16], consider shell convergence with zero pressure on the inner boundary and $f(t) = U_{B0} r_{B0}^2 = const$. At time t0, the radius and velocity of the inner boundary, r_{B0} and $U_{B0} < 0$, are defined. In accord with (17) at time t_0, velocity depends on radius

$$U = U_{B0} (r_{B0}/r)^2. \tag{21}$$

Let all quantities on the outer boundary be subscripted "a". Assume that the shell mass is equal to M_a. The coordinate of the outer boundary, ra, relate to that of the inner boundary r_B as $r_a = \left(r_B^3 + b\right)^{1/3}$, where $b = \frac{3V_0}{4\pi} M_a = r_{a0}^3 - r_{B0}^3$. Pressure and velocity on the outer boundary are

$$U_a = U_{B0} \left(\left(\frac{r_{a0}}{r_{B0}} \right)^3 - \frac{t - t_0}{t_f - t_0} \right)^{-2/3}, \tag{22}$$

$$P_a = \frac{U_{B0}^2}{2V_0} \left(\left(\frac{t_f - t}{t_f - t_0} \right)^{-4/3} - \left(\left(\frac{r_{a0}}{r_{B0}} \right)^3 - \left(\frac{t - t_0}{t_f - t_0} \right) \right)^{-4/3} \right). \tag{23}$$

The values U_{a0} and P_{a0} are found from (22) and (23) at $t = t_0$. In Lagrangian coordinates the pressure, velocity and released energy are defined by

$$P = \frac{U_{B0}^2}{2V_0} \left(\left(\frac{t_f - t}{t_f - t_0} \right)^{-4/3} - \left(\frac{t_f - t}{t_f - t_0} + \frac{3V_0 M}{4\pi r_{B0}^3} \right)^{-4/3} \right),$$

$$U = U_{B0} \left(\frac{t_f - t}{t_f - t_0} + \frac{3V_0 M}{4\pi r_{B0}^3} \right)^{-2/3}, \tag{24}$$

$$\frac{\partial q}{\partial t} = \frac{2U_{B0}^3}{\Gamma r_{B0}} \left(\left(\frac{t_f - t}{t_f - t_0} + \frac{3V_0 M}{4\pi r_{B0}^3} \right)^{-7/3} - \left(\frac{t_f - t}{t_f - t_0} \right)^{-7/3} \right).$$

As the reference problem we consider the motion of 10% shell.

Problem 6. The motion of a 10%-shell. At $t_0 = 0$, $r_{B0} = 1$, $r_{a0} = 1.1$, $V_0 = 1$, and $M_a = 1.38649$. The velocity of the inner boundary is $U_{B0} = 1$. The EOS of shell material with parameters $\rho_{0k} = 1$, $C_{0k} = 1$ and $\Gamma = 2$ has the form $P = 2\rho E + \rho - 1$. At the initial time, pressure, specific internal energy and velocity in the shell are defined by

$$P(M) = 1 - \left(1 + \frac{3M}{4\pi}\right)^{-4/3}, \qquad E(M) = \frac{1}{4}\left(1 - \left(1 + \frac{3}{4\pi}\right)^{-4/3}\right),$$

$$U = U_{B0}\left(\frac{4\pi r_{B0}^3 \rho_0}{3M}\right)^{2/3}.$$

Boundary conditions: at $t \geq 0$, $P_B = 0$, $M_B = 0$, $U_a = -\left(1, 1^3 - 3t\right)^{-2/3}$ at $t \geq 0$, $M = M_a$. From (20) we found $t_f = 1/3$. At $t \geq 0$, energy release as a function of t and M is defined by

$$\frac{dq}{dt} = \left(1 - 3t + \frac{3M}{4\pi}\right)^{-7/3} - (1 - 3t)^{-7/3}.$$

For $t \geq 0$ and $M_a \geq M \geq 0$ the solution has the form

$$E(t, M) = \frac{1}{4}\left((1 - 3t)^{-4/3} - \left(1 - 3t + \frac{3M}{4\pi}\right)^{-4/3}\right), \qquad P = 2E, \quad \rho = 1,$$

$$U(t, M) = -\left(1 - 3t + \frac{3M}{4\pi}\right)^{-2/3}.$$

Figures 11 and 12 show pressure and velocity as functions of $m = M/M_a$ at $t_1 = 0,30$, $t_2 = 0,32$.

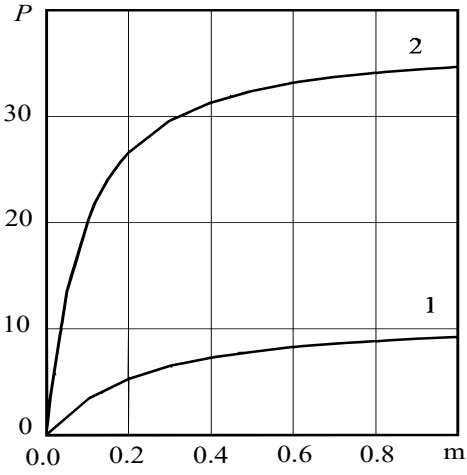

Fig. 11. Problem 6.
$P(m)$ at $t_1 = 0.3$ (line 1) and $t_2 = 0.32$ (line2)

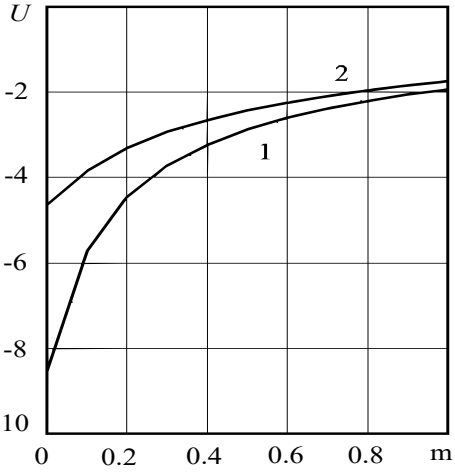

Fig. 12. Problem 6.
$U(m)$ at $t_1 = 0.3$ (line 1) and $t_2 = 0.32$ (line2)

4 Shock in a gas sphere

In different years, there were published a number of papers [18-22] with self-similar solutions to shock convergence in infinite ideal gas. Shock convergence in a gas sphere of finite radius is considered in [23,24]. At $t = t_0$, pressure in gas is $P_0 = 0$, density $\rho_0 = const$, velocity $U_0 = 0$, and specific internal energy $E_0 = 0$. The boundary of the sphere is at a point (r_0, t_0). Velocity on the boundary is $U_{g0} < 0$. In other words, velocity jumps on the boundary, producing a shock wave which moves into the sphere. At the time when the shock converges, t_f, its coordinate r_w is zero. The equation of motion which satisfies all these conditions is

$$r_w = r_0 \left(\frac{t_f - t}{t_f - t_0} \right)^n \tag{25}$$

for $n > 0$ Its differentiation gives shock velocity

$$D = D_0 \left(\frac{t_f - t}{t_f - t_0} \right)^{n-1}, \tag{26}$$

where

$$D_0 = -r_0 n \Big/ \left(t_f - t_0 \right). \tag{27}$$

Flow parameters are defined by

$$\begin{gathered} \frac{\partial \rho}{\partial t} + U \frac{\partial \rho}{\partial r} + \rho \frac{\partial U}{\partial r} + \frac{2\rho U}{r} = 0, \\ \frac{\partial U}{\partial t} + U \frac{\partial U}{\partial r} + \frac{1}{\rho} \frac{\partial P}{\partial r} = 0, \\ \frac{\partial P}{\partial t} + U \frac{\partial P}{\partial r} + \gamma P \left(\frac{\partial U}{\partial r} + \frac{2U}{r} \right) = 0. \end{gathered} \tag{28}$$

For solving the problem we change from the variables t and r to variables t and $\xi(t, r)$. The function $\xi(t, r)$ is taken such as to remain constant on the shock. Its simplest form reads as

$$\xi = \frac{r}{r_0} \left(\frac{t_f - t_0}{t_f - t} \right)^n. \tag{29}$$

Now express P, ρ and U as functions of time multiplied by functions of ξ:

$$P = \alpha_p(t)\, \Pi(\xi), \quad \rho = \alpha_\rho(t)\, \delta(\xi), \quad U = \alpha_u(t)\, \mathrm{M}(\xi). \tag{30}$$

Choose $\Pi(\xi)$, $\delta(\xi)$, $M(\xi)$ such that to allow them at $\xi = 1$ take the values

$$\delta_w = \frac{\gamma + 1}{\gamma - 1}, \quad \mathrm{M}_w = \frac{2}{\gamma + 1}, \quad \Pi_w = \frac{2}{\gamma + 1}. \tag{31}$$

With these δ_w, Π_w, M_w the function α_ρ, α_u and α_p take the forms

$$\alpha_\rho = \rho_0, \quad \alpha_u = D_0 \left(\frac{t_f - t_0}{t_f - t} \right)^{1-n}, \quad \alpha_p = \rho_0 D_0^2 \left(\frac{t_f - t_0}{t_f - t} \right)^{2(1-n)}. \tag{32}$$

After appropriate manipulation for conversion to the functions Π, δ, M and variables t, ξ, we obtain equations for functions which only depend on ξ:

$$(\mathrm{M} - \xi)\,\delta' + \delta \mathrm{M}' + \frac{2\mathrm{M}\delta}{\xi} = 0, \qquad \frac{n-1}{n}\delta \mathrm{M} + \mathrm{M}'\delta\,(\mathrm{M} - \xi) + \Pi' = 0, \tag{33}$$

$$\frac{2\,(n-1)}{n}\Pi + \Pi'\,(\mathrm{M} - \xi) + \gamma \Pi \mathrm{M}' + \frac{2\gamma \mathrm{M}\Pi}{\xi} = 0. \tag{34}$$

For M', δ', Π' , these equations give a system of linear homogeneous equations. If its determinant

$$Z = (\mathrm{M} - \xi)\left(\gamma \Pi - \delta\,(\mathrm{M} - \xi)^2\right) \tag{35}$$

is nonzero, the system has a unique solution. At the point ξ_* where $Z = 0$, the matrix of coefficients and the augmented matrix of coefficients should be considered. At this point their ranks are identical and equal to 2, and all third-order minors are zero, hence the system of equations (33) and (34) has a unique solution. It is easy to show that with the zero third-order minors we come to

$$(n-1)\,\xi_*\,(2\,(\mathrm{M}_* - \xi_*) - \gamma \mathrm{M}_*) + 2\gamma n \mathrm{M}_*\,(\mathrm{M}_* - \xi_*) = 0. \tag{36}$$

The value of n is found from the condition that equation (36) holds simultaneously with

$$Z_* = (\mathrm{M}_* - \xi_*)\left(\gamma \Pi_* - \delta_*\,(\mathrm{M}_* - \xi_*)^2\right) = 0. \tag{37}$$

From equations (36) and (37) we find the appropriate values of n for each γ. This solution was used to evaluate the accuracy of some shock calculation methods.

Problem 7. A cold gas sphere of radius $r_{g0} = 1$ with parameters $P_0 = 0$, $\rho_0 = 1$, $U_0 = 0$, $U_{g0} = 1$, $\gamma = 5/3$. The boundary condition is defined through reverse transition from t, ξ and Π, δ, M to t, M and P, ρ, U. Pressure and boundary velocity as functions of time are presented in Table 1. Pressure, density and velocity profiles at $t = 0.4, 0.45, 0.5$ (marked 1, 2, 3) are shown in Figs. 13-15. The solid lines show the analytical solution derived in this work, the lines with circles show calculations by the VOLNA code [25] with no shock smearing, and the dashed lines show VOLNA calculations with shock smearing. The calculations were done on a uniform mesh of 100 points in r at $t = t_0$. In Fig.14, entropy traces are seen in the dashed density profiles, which are a result of shock smearing on the boundary. Figure 16 depicts $M(\xi)$, (ξ) and $\delta(\xi)$ for $1 \le \xi \le 5$.

Table 1.

Problem 7. The boundary condition in the case of $\gamma = 5/3$

No.	t	U	P	No.	t	U	P
1	0	-1.00000	1.333333	17	0,30	-1.045146	2.445445

Table 1. Continuation.

No.	t	U	P	No.	t	U	P
2	0.04	-1.008791	1.415094	18	0,31	-1.044921	2.517083
3	0.07	-1.015161	1.484529	19	0,32	-1.044473	2.592849
4	0.10	-1.021256	1.562232	20	0,33	-1.043787	2.673060
5	0.13	-1.026982	1.649664	21	0,34	-1.042842	2.758063
6	0.16	-1.032224	1.748622	22	0,35	-1.041619	2.848236
7	0.18	-1.035380	1.822074	23	0,36	-1.040097	2.943996
8	0.20	-1.038211	1.902413	24	0,37	-1.038251	3.045798
9	0.22	-1.040657	1.990554	25	0,38	-1.036058	3.154141
10	0.23	-1.041717	2.037877	26	0,39	-1.033488	3.269573
11	0.24	-1.042655	2.087565	27	0,40	-1.030514	3.392698
12	0.25	-1.043463	2.139778	28	0,42	-1.023220	3.664748
13	0.26	-1.044129	2.194694	29	0,45	-1.008354	4.149469
14	0.27	-1.044643	2.252502	30	0,50	-0.969947	5.233492
15	0.28	-1.044992	2.313410	31	0,55	-0.899013	6.144230
16	0.29	-1.045165	2.377642				

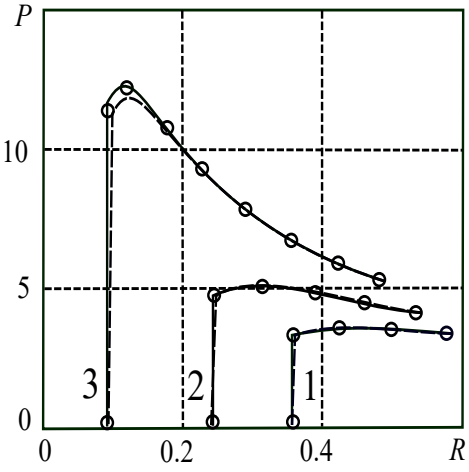

Fig. 13. Problem 7. pressure profiles at times 0.4 (1), 0.45 (2), 0.5 (3)

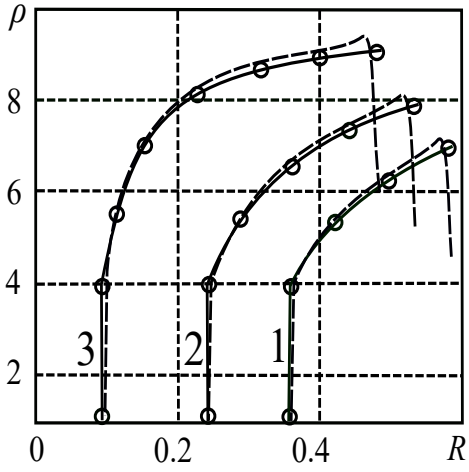

Fig. 14. Problem 7. density profiles at times 0.4 (1), 0.45 (2), 0.5 (3)

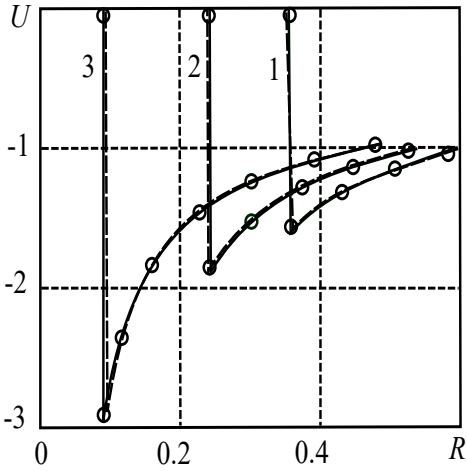

Fig. 15. Problem 7. velocity profiles at times 0.4 (1), 0.45 (2), 0.5 (3)

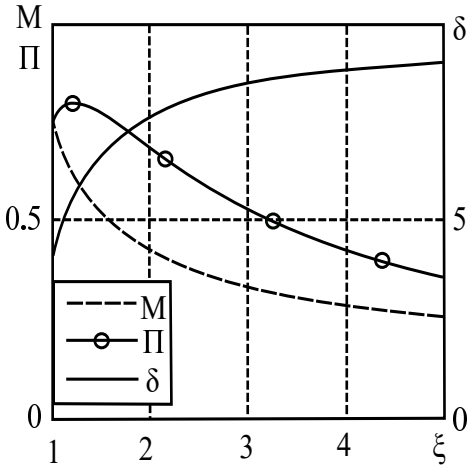

Fig. 16. Problem 7. profiles of dimensionless M(ξ), $\Pi(\xi)$, $\delta(\xi)$

References

1. P.D. Lax and R.D. Richtmyer, Survey of stability of linear finite difference equations. Commun. Pure and Appl. Math. – 1956 – V. 9 – P. 267–293.
2. P.J. Roach, Computational Fluid Dynamics. Albuquerque: Hermosa Publishers, 1976.
3. V.F. Kuropatenko, and I.R. Makeyeva, Investigation of discontinuity distraction in shock calculation methods. J. Mathematical Modeling – 2006 – . 18 – No. 3 – P. 120–128.
4. J. von Neumann, and R.D. Richtmyer, A method for the numerical calculation of hydrodynamic shocks. Appl. Phys. – 1950 – V. 21 – No. 3 – P. 232–237.
5. M.L. Wilkins, Simulation of elastic-plastic flows. In Computational Methods in Hydrodynamics, Moscow, MIR Publishers, 1967, P. 212–263.
6. A.A. Samarsky, and V.Y. Arsenin, Numerical solution of hydrodynamic equations with different viscosities. J. Comp. Math. and Mathem. Phys. – 1961 – V. 1 – No. 2 – P. 357–380.
7. V.F. Kuropatenko, A pseudo-viscosity form. Transactions of the Siberian Branch of USSR Academy of Sciences – 1967 – No. 3 – Is. 3 – P. 81–82.
8. V.F. Dyachenko, Numerical analysis of discontinuous solutions to quasi-linear systems. J. Comp. Math. and Mathem. Phys. – 1961 – V. 1 – No. 6 – P. 1127–1129.
9. V.F. Kuropatenko, and Y.N. Andreyev, Simulation of dynamic processes in spherical and cylindrical shells. J. Computational Continuum Mechanics – 2010 – V. 3 – No. 4 – P. 53–67.
10. V.F. Kuropatenko, A shock capture method. SUSU Bulletin, Mathematical Modeling and Programming Series – 2014 – V. 7 – No. 1 – P. 62–75.
11. V.F. Kuropatenko, A shock calculation method. Proceedings of USSR Academy of Sciences – 1960 – V. 3 – No. 4 – P. 771–772.
12. V.F. Kuropatenko, I.A. Dorovskikh, and I.R. Makeyeva, The influence of difference scheme properties on mathematical modeling of dynamic processes. J. Computing Technologies – 2006 – V. 11 – Part 2 – P. 9–11.
13. V.F. Kuropatenko, and M.N. Yakimova, A Method of Shock Calculation. J. Computational and Engineering Mathematics – 2015 – V. 2 – No. 2 – P. 60–70.

14. E.I. Zababakhin, Energy cumulation and its bounds. J. Achievements in Physics – 1965 – V. 85 – Is. 4 – P. 721–726.
15. K.V. Brushlinsky, and Y.M. Kazhdan, On self-similar solutions to some hydrodynamic problems. J. Achievements in Mathematics – 1963 – V. 18 – No. 2 – P. 3–23.
16. V.F. Kuropatenko, Collapse of spherical cavities and energy cumulation in compressible ideal fluid. J. Combustion and Detonation Physics – 2015 – V. 51 – No. 1 – P. 57–65.
17. V.F. Kuropatenko, Equations of state for low-temperature dense plasma components. Encyclopedia of Low-temperature Plasma – B Series – V. VIII – Part 2 – Moscow: JANUS-K Publishers – 2008 – P. 436–450.
18. G. Hunter, On the collapse of an empty cavity in water. J. Fluid Mechan. – 1960 – V. 8 – No. 2 – P. 241–263.
19. L.I. Sedov, Unsteady flows of compressible fluid. Proceedings of USSR Academy of Sciences – 1945 – V. 47 – No. 2 – P. 94–96.
20. K.P. Stanyukovich, Self-similar solutions to hydrodynamic equations with central symmetry. Proceedings of USSR Academy of Sciences – 1945 – V. 48 – No. 5 – P. 331–333.
21. A.N. Krayko, Fast cylindrically and spherically symmetric strong compression of ideal gas. J. Applied Mathematics and Mechanics – 2007 – V. 71 – No. 5 – P. 774–760.
22. S.P. Bautin, Mathematical modeling of strong gas compression. Novosibirsk, Nauka Publishers, 2007.
23. V.F. Kuropatenko, E.S. Shestakovskaya, and M.N. Yakimova, Dynamic compression of a cold gas sphere. Proceedings of Academy of Sciences – 2015 – V. 461 – No. 5 – P. 530–532.
24. V.F. Kuropatenko, E.S. Shestakovskaya, and M.N. Yakimova, Shock in a gas sphere. SUSU Bulletin Mathematical Modeling and Programming Series – 2015 – V. 8 – No. 4 – P. 14–29.
25. V.F. Kuropatenko, V.I. Kuznetsova, G.V. Kovalenko, G.I. Mikhaylova, and G.N. Sapozhnikova, VOLNA code and an inhomogeneous difference technique for unsteady flows of compressible continua. J. Problems in Nuclear Science and Technology – Mathematical Modeling of Physical Processes Series – 1989 – Is. 2 – P. 9–25.